Au thin-film electrodes based potentiometric CO_2 sensor using Li_3PO_4 as both the reference material and the solid electrolyte

Hairong Wang[1,2] ✉, *Di Chen*[1,2], *Zhen Liu*[1,2], *Mi Zhang*[1,2]

[1]*School of Mechanical Engineering, Xi'an Jiaotong University, Xi'an 710049, People's Republic of China*
[2]*State Key Laboratory for Manufacturing Systems Engineering, No. 99 Yan Cheung Road, Xi'an 710054, People's Republic of China*
✉ *E-mail: whairong@mail.xjtu.edu.cn*

Published in Micro & Nano Letters; Received on 1st May 2016; Revised on 19th June 2016; Accepted on 20th June 2016

Thin-film Au electrodes prepared by magnetron sputtering method were used to develop a potentiometric CO_2 gas sensor. The thermal evaporated Li_3PO_4 played the role of electrolyte and sensing material. This design can simplify the fabrication process compared with the conventional solid electrolyte potentiometric CO_2 sensor (c-sensor) and improve the performance compared with the thick-film Au electrodes sensor (t-sensor). The designed CO_2 sensor (d-sensor) presented good response characteristics at the CO_2 concentration range of 250–2500 ppm and the electromotive force (EMF), ΔEMF/dec, response and recovery time were investigated. The EMF values of the sensor were linearly dependent on logarithm of CO_2 partial pressure at the working temperatures between 420°C and 500°C. The d-sensor showed a sensitivity of 79.1–93.7 mV/dec at working temperatures range of 420–500°C which was much higher than the sensitivities of c-sensor and the t-sensor. The response and recovery time of the fabricated sensors were 10 and 14 s at working temperature of 500°C, respectively. The surface morphology of Au thin films was considered to increase the three-phase interface area and be good for the reaction gases to diffuse from Au film to lithium phosphate, allowing rapid chemical reaction equilibrium, getting a more stable EMF output.

1. Introduction: In recent decades, especially since the industrial revolution, the concentration of carbon dioxide in the atmosphere has increased approximately by 30% due to vehicle emissions and the burning of fossil fuels [1]. Because of rapid increase of carbon concentration and fast deterioration of people's living environments, requirement for the detection and control of carbon dioxide has been increasing. So far, many types of carbon dioxide sensors have been reported, including infrared [2], capacitive [3], resistive [4] and solid electrolyte [5–19]. Solid electrolyte type sensor based on electrochemical principle has been widely studied due to its higher sensitivity, selectivity and lower power consumption. Therefore, various kinds of electrolytes have been used to fabricate CO_2 sensors, including YSZ [7], NASICON [8], LaF [3, 9], Li_3PO_4 [10–12], and lithium phosphorous oxynitride [13]. Among them, CO_2 sensors based on Li_3PO_4 are promising due to their faster response and lower water reactive nature than any other alkali ion conducting materials [14].

However, solid electrolyte CO_2 sensor based on Li_3PO_4 always presents a lower sensitivity (ΔEMF/dec) than the theoretical value [15]. So far, researchers have tried many methods to improve sensor's sensitivity. When the polished alumina substrate was used in Li Peng's paper, the sensitivity of fabricated sensor was 55 mV/dec compared with 45 mV/dec on roughness substrate at 500°C operating temperature [16]. However, the improved sensitivity was still far less than the theoretical value. The relationship between the thickness of the electrolyte and the sensitivity of the sensor has been investigated [15]. When the thickness of Li_3PO_4 thin film was 1.2 μm, a sensitivity of 61 mV/dec has been obtained at 500°C operating temperature, which was about 80% of the theoretical value. The deviation of sensitivity can contribute to different compositions of c-sensor usually cannot achieve ideal activation energy state at the same temperature. In order to reduce the reaction area and simplify the fabrication process, some researchers reported that the reference material can be omitted. According to Lee *et al.*, [17] lithium phosphate can serve as both the reference and the solid electrolyte material. In the structure of the proposed sensor, the Au electrodes for reference side and sensing side were screen-printed and fired at 700–800°C. Furthermore, a Li-ion based stacked-type potentiometric solid-state sensor using thick Au film has been designed and fabricated to reduce the active area and simplify the fabrication process [18]. As discussed above, the thickness of the Au electrodes fabricated by thick-film technology was few micrometres. In order to further improve the performance of the sensor, an Au thin film electrodes based CO_2 sensor was proposed in this Letter.

In this Letter, we designed an Au thin-film based CO_2 sensor. Li_3PO_4 film fabricated by thermal evaporation method played the role of solid electrolyte and reference material. Au thin film electrodes were prepared by sputtering method with thickness of few hundred nanometres. The sensing electrode was fabricated by screen printing method. The electromotive force (EMF), ΔEMF/dec, response and recovery time were investigated at various temperatures and gas concentrations.

2. Experimental details: Schematic diagram of the conventional planar CO_2 sensor (c-sensor) and designed CO_2 sensor in our Letter (d-sensor) are shown in Fig. 1. The structure of the thick-film sensor is similar to the d-sensor except the thickness of Au electrodes fabricated by screen printing method. A polished alumina plate was used as a rigid substrate of the sensor. The dimension of the Al_2O_3 substrate was $3 \times 4 \times 0.625$ mm. The fabrication process of the d-sensor was as follows. A Li-ion conductor (99.9% Li_3PO_4) was deposited on the alumina substrate by thermal evaporation method (ZHD-400 Resistance Evaporation Coating Machine, Technol Science, Beijing, China) with a thickness of 1.2 μm and a deposition velocity of 3.3 A°/s. Thermal evaporation voltage, current and working pressure were 4.5 V, 213 A, and 3×10^{-3} Pa, respectively. The as-deposited thin films were sintered at 700°C for 2 h in a tubular furnace (HTL1000-80) with a heating rate of 5°C/min under the air atmosphere. Thin Au films as the two metal electrodes of the sensor were sputtered on the solid electrolyte film at a deposition velocity of 20 nm/min by using magnetron sputtering method (Explorer 14, Denton Vacuum America) to a thickness of 400 nm. The Au electrodes were sputtered by using mechanical Al_2O_3 mask and without subsequent heat treatment. Moreover,

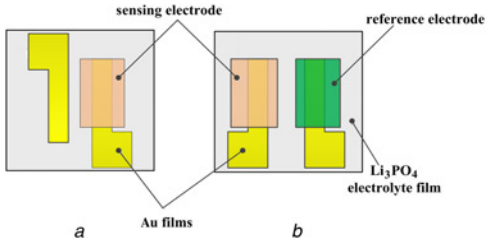

Fig. 1 *Schematic diagram of the CO_2 sensor*

for the thick-film sensor (t-sensor), the Au electrodes were screen-printed onto the annealed Li_3PO_4 film with a thickness of 20 μm, followed by a 700°C annealing for 1 h. Next, to make the paste-type material used in screen printing process, Li_2CO_3 powder (Sinopharm Chemical Reagent Company Limited, 99.99%) was mixed with organic vehicle consisting of alpha-terpineol and ethyl cellulose. Then the paste was printed on the two kinds of Au electrodes and sintered at 600°C for 1 h with a heating rate of 5°C/min under the air atmosphere. As for the c-sensor, after the above steps were finished, Li_2TiO_3 (Aldrich, 99.99%) mixed with organic vehicle was printed on the Au electrode and fired at 700°C for 1 h. Pt wires were attached on the gold electrodes and annealed at 500°C for 30 min to make good contact. Finally, for the measurement of the properties of the sensors, 5000 ppm CO_2 and synthetic air were used to prepare different concentrations of CO_2 gases (250–2500 ppm) via a gas distribution system. In the system, two mass flow controllers connected to a computer were used to prepare a series of different concentrations of CO_2 gas. The total flow rate of the gases was set as 200 sccm. The fabricated gas sensors were tested in a steel chamber and in a tubular furnace (HTL1000-80) which temperature could be precisely controlled. The sensing characteristics of the sensors to CO_2 were investigated at a temperature range from 380°C to 520°C. The EMF was collected by an electrometer (Keithley 6517B).

3. Results and discussions: At the sensing electrode, the electrochemical reaction is denoted by (1). On the reference electrode side, due to the absence of reference material, the lithium ions of Li_3PO_4 are supposed to react only with oxygen [19], as shown in (2). The total reaction between the reference electrode and sensing electrode can be described by (3).

$$Li_2CO_3 \Leftrightarrow Li^+ + CO_2 + \frac{1}{2}O_2 + 2e^- \quad (1)$$

$$2Li^+ + \frac{1}{2}O_2 + 2e^- \Leftrightarrow Li_2O \quad (2)$$

$$Li_2O + CO_2 \Leftrightarrow Li_2CO_3 \quad (3)$$

$$E = \frac{\Delta G^{\Theta}}{nF} + \left[\frac{RT}{nF}\right] \ln\left[a_{Li_2O}\right] + \left[\frac{RT}{nF}\right] \ln\left[p_{CO_2}\right] \quad (4)$$

$$E = E^0 + \left[\frac{RT}{nF}\right] \ln\left[p_{CO_2}\right] \quad (5)$$

According to reaction (1) and (2), the EMF of the sensor follows (4). ΔG^{Θ} is the Gibbs free energy of the reaction (3) at the operating temperature, a_{Li_2O} the activity of lithium oxide at the reference electrode interface, p_{CO_2} the carbon dioxide partial pressure, R the universal gas constant, n the number of reaction electrons and F the Faraday constant. Under the condition that activity of lithium oxide is constant; the EMF of the sensor follows (5). E^0 is a certain value in a given working environment for a certain kind of sensor, the EMF is mainly determined by the working temperature T and the partial pressure of CO_2 (p_{CO_2}).

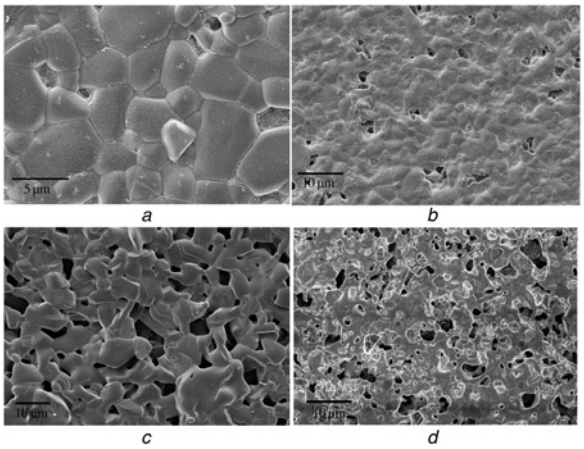

Fig. 2 *SEM images*
a Li_3PO_4 film
b Thin film Au electrode
c Sensing Li_2CO_3
d Thick film Au electrode

According to reaction (1) and (2), the number of transmission reaction electrons should be 2. On the basis of formula (5), the absolute value of EMF increases logarithmically or linearly with the concentration of carbon dioxide decrease or the operating temperature increase, respectively.

The surface morphology of the electrolyte, sensing material, thin Au film electrode and thick Au film electrode are shown in Fig. 2. The photograph of the Li_3PO_4 film in the figure shows the morphology after a heat treatment at 700°C for 2 h. The magnification of the Li_3PO_4 film, Au electrodes and sensing material are 5, 1 and 1.5 K, respectively. The scanning electron microscope (SEM) image indicates Li_3PO_4 film was dense, crystalline and continuous. Li_3PO_4 grain and grain boundary is clearly visible, at the same time due to the growth of the grain and mutual extrusion, Li_3PO_4 grains present the approximate polygonised structure. The particle size is mostly around 4 μm. All of these factors were considered to be advantage of the transference of lithium ion. According to Fig. 2*b*, the sputtered gold electrode's surface was denser and smoother compared with the screen painted Au electrode. Fig. 2*c* shows the SEM image of the printed Li_2CO_3 sensing electrode after annealed at 600°C for 1 h. The thick film presents a porous morphology with grain sizes about 5–20 μm. Normally, for thick film gold electrode, the reaction gases are difficult to diffuse through the electrode and the three-phase interface should mostly occur at the periphery of the electrode. However, according to Fig. 2*b*, the Au film spreads holes with diameter of about 5 μm, and in view of that the thin film electrode thickness is only 400 nanometers and the porous morphology of the Li_2CO_3 sensing electrode, these holes can be considered to increase the three-phase interface area at sensing electrode and be good for the reaction gas to diffuse from Au film to lithium phosphate, allowing rapid chemical reaction equilibrium. The Au thin-film electrodes were prepared by magnetron sputtering method with a dense and smooth surface that can make good contact with the Li_3PO_4 film and maintain good electrical conductivity at the same time. Oxygen gas can diffuse into the lithium phosphate easily both at the sensing and the reference side due to the porous surface. All these features can be considered to improve the performance of the d-sensor.

As shown in Fig. 3*a*, the d-sensor showed a much higher initial EMF value and a better transient property than the c-sensor and t-sensor. As the operating temperature was increased, the ΔEMF of both d-sensor and c-sensor also increased but not the t-sensor. The ΔEMF of t-sensor in Fig. 3 increases from 420 to 440°C but decreases from 460 to 500°C. Li_2O in electrochemical reaction

doi: 10.1049/mnl.2016.0240

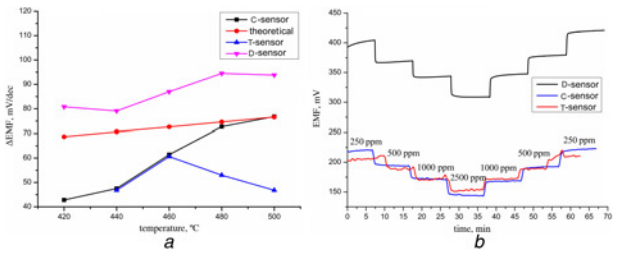

Fig. 3 *Dependence of theoretical and experimental ΔEMF/dec as a function of working temperature and response transients of the d-sensor, c-sensor and t-sensor to various CO_2 concentrations at 500°C*
a Theoretical and experimental ΔEMF/dec
b Response transients

(2) is supposed to build in situ at the interface of gold electrode and Li_3PO_4 film. In view of thickness difference between the screen painted thick Au film and the thermal evaporated Li_3PO_4 film, the contact between Au film and Li_3PO_4 film was poor and may deteriorate when the working temperature increasing due to the thermal stress. The poor contact is considered to be bad for the chemical reaction equilibrium which can cause the decreases of ΔEMF of t-sensor.

The response and recovery characteristics of the d-sensor in the CO_2 concentration range from 250 to 2500 ppm at different working temperatures are shown in Fig. 4. In the figure, the high and low volt represented the EMF of the sensor in the CO_2 concentration of 250 and 2500 ppm. To obtain the stable EMF value, the duration time of CO_2 concentration was set as 10 min. The d-sensor presented good response and recovery characteristics even when the operating temperature was 380°C. Fig. 5 shows the response transients of the d-sensor at the operating temperature of 380, 400, 420, 440, 460, 480, 500 and 520°C. To test the response characteristics of the d-sensor, a gas distribution system was used to inject the test gas every 10 min. The injected gas concentrations were 250, 500, 1000 and 2500 ppm in sequence and then reversed. The flow rates of the balance and target gases were both 200 sccm. The results indicated that the fabricated sensor was sensitive to CO_2 under the test condition. It can be seen from the figure that the EMF values were pretty stable in the test interval. The EMF was inversely proportional to the logarithm of concentration of carbon dioxide and proportional to the operating temperature, respectively.

Figs. 6 and 7 show the dependence of EMF as a function of CO_2 concentration at the working temperature range of 380–520°C for t-sensor and d-sensor. It can be found that the EMF values were much linear to the logarithm of CO_2 concentration as expressed

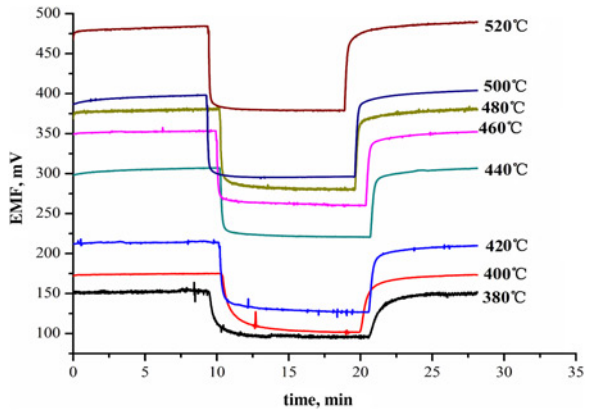

Fig. 4 *Response and recovery characteristics of the d-sensor at the CO_2 concentration range from 250 to 2500 ppm at different working temperatures*

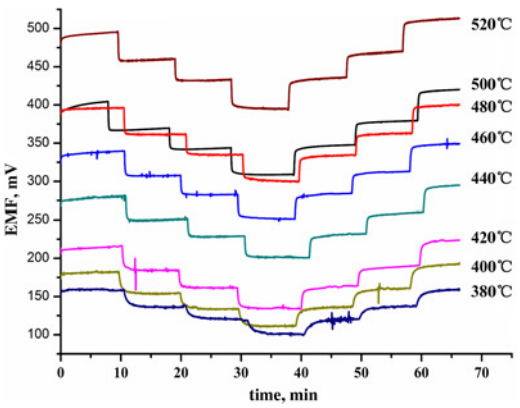

Fig. 5 *Response transients of d-sensor to various CO_2 concentrations at temperature range of 380–520°C*

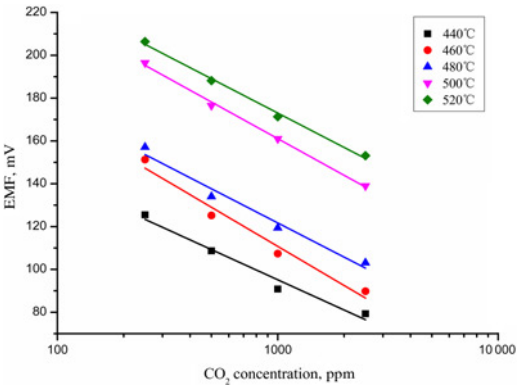

Fig. 6 *EMF of t-sensor against logarithmic CO_2 concentrations at the working temperature range of 440–520°C*

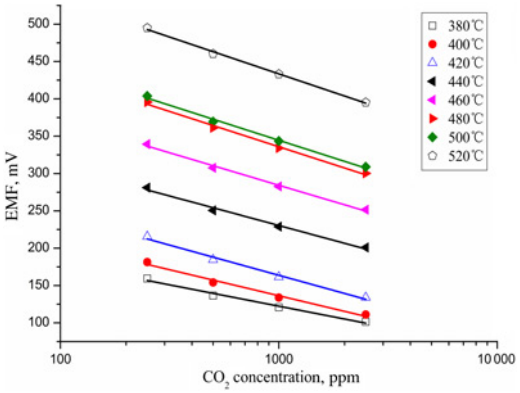

Fig. 7 *EMF of d-sensor against logarithmic CO_2 concentrations at the working temperature range of 380–520°C*

by (4). In the temperature range from 380°C to 520°C, the initial EMF of d-sensor increased with enhancement of working temperature. Fig. 8 shows the dependence of ΔEMF/dec as a function of operating temperature for the d-sensor. The theoretical sensitivity can be calculated from the equation $-2.3(RT/nF)$. It can be seen from Fig. 8 that the ΔEMF values were increased up to 520°C operating temperature and were much higher than the theoretical values except at 380°C. The sensitivity of sensor was very low at 380°C, this can be attributed to the effect of low kinetic energies produced between each electrode and the low ionic conductivity

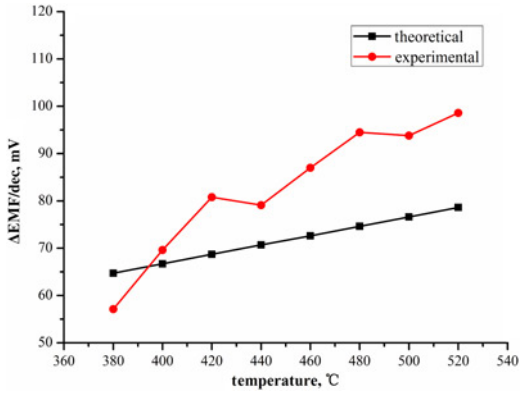

Fig. 8 *Dependence of theoretical and experimental ΔEMF/dec as a function of working temperature*

Table 1 Electron transfer number '*n*' calculated from Fig. 7

Temperature	400	420	440	460	480	500	520
value of '*n*'	1.90	1.70	1.79	1.67	1.58	1.64	1.60

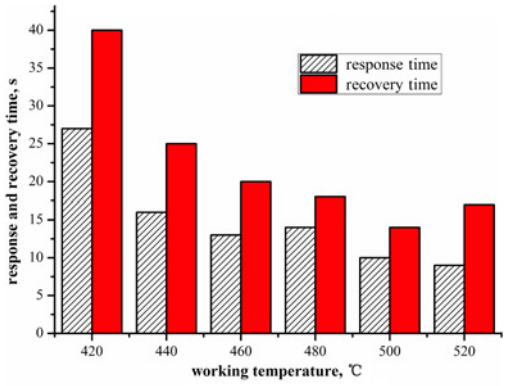

Fig. 9 *Response and recovery time of the sensor at different working temperatures*

of the electrolyte at low temperature and reaching a non-equilibrium state [16].

To investigate the relationship between the sensitivity and the electron transfer number '*n*', we only analysed the theoretical sensitivity determined by (5) and experimental sensitivity at the working temperature range from 400°C to 520°C, as shown in Table 1. The number of electron transferred in the experiment calculated from the fitting line in Fig. 7 was less than the theoretical value of 2, but the causes of this phenomenon still need to be further researched.

Fig. 8 shows the dependence of theoretical and experimental ΔEMF/dec of d-sensor as a function of working temperature. The response and recovery time is an important factor of solid electrolyte sensor. In order to confirm the usefulness of the sensor designed in this Letter, the response and recovery time were obtained at a CO_2 concentration curve from 500 to 1000 ppm at different working temperatures as shown in Fig. 9. Response and recovery time were defined as the 90% time interval that the sensor took to equilibrate from one equilibrium state to another when the concentration of CO_2 was changed. Fig. 9 indicates that the response and recovery time reduced with the increase of the working temperature but reached a plateau between 480–520°C. The response and recovery times calculated at 500°C were around 10 and 14 s, respectively. Furthermore, Fig. 9 also shows that response and recovery time were 16 and 25 s even when the working temperature was 440°C. It can be seen from Fig. 8 that the ΔEMF value was 79.1 mV/dec at 440°C that can meet the requirement of applications. Compared with the prevalent 500°C working temperature, the power consumption can be reduced without losing high sensitivity. However, clear explanation about the sensitivity still need to be investigated in future research.

The fabricated sensor showed a batter performance in sensing CO_2 gas compared with the sensors using thick-film Au electrode. This can attribute to the thin film may be easier to get high activation energy at a relatively lower temperature on the one hand and large three-phase interface area caused by the holes spread on the Au electrode on the other. Furthermore, the reaction gas can be easier to diffuse from Au thin-film electrode to lithium phosphate, this can accelerate the reaction rate. It proved that the thin-film Au electrodes can be used to improve the sensitivity of potentiometric CO_2 sensors.

4. Conclusion: A potentiometric CO_2 sensor based on Au thin film electrodes was designed and fabricated. The thermal evaporated Li_3PO_4 played the role of electrolyte and sensing material. The surface morphology of fabricated Au electrode was considered to increase the area of the three-phase and be good for the reaction gases to diffuse to the three-phase interface. The fabricated sensors were characterised using SEM, and were tested at the CO_2 concentration range of 250 to 2500 ppm. The response and recovery times of the d-sensors were 10 and 14 s at working temperature of 500°C, respectively. The EMF values of d-sensor were logarithmic dependent on the CO_2 partial pressure between 250 and 2500 ppm at the working temperature range of 380–520°C and were pretty stable in the test interval. The ΔEMF/dec values increased with working temperature and were 69.6–98.6 mV/dec at working temperatures range of 400 to 520°C which was much higher than that of c-sensor and t-sensor. The d-sensor can work at low power consumption with high sensitivity and fast response which is adaptable to ubiquitous sensor applications.

5. Acknowledgments: The work was supported by Natural Science Foundation of China (grant no. 51175416), Major National Science and Technology Projects of China (grant nos. 2013ZX03005007 and 2011ZX04004-061), the Basic Scientific Research Expenses of Central University (grant no. xjj2014105), and Science and Technology Program of Shaanxi Province (grant no. 2014K05-01).

6 References

[1] Fan K., Qin H., Wang L., Ju L., Hu J.: 'CO_2 gas sensors based on La1−xSrxFeO$_3$ nanocrystalline powders', *Sens. Actuators B*, 2013, **177**, pp. 265–269

[2] Hodgkinson J., Smith R., Ho W.O., Saffell J.R., Tatam R.P.: 'Non-dispersive infra-red (NDIR) measurement of carbon dioxide at 4.2 m in a compact and optically efficient sensor', *Sens. Actuators B*, 2013, **186**, pp. 580–588

[3] Lee H.J., Park K.K., Kupnik M., Khuri-Yakub B.T.: 'Functionalization layers for CO_2 sensing using capacitive micromachined ultrasonic transducers', *Sens. Actuators B*, 2012, **174**, pp. 87–93

[4] Trung D.D., Toan L.D., Hong H.S., Lam T.D., Trung T., Hieu N.V.: 'Selective detection of carbon dioxide using LaOCl-functionalized SnO_2 nanowires for air-quality monitoring', *Sens. Actuators B*, 2012, **88**, pp. 152–159

[5] Pasierb P., Rekas M.: 'Solid-state potentiometric gas sensors current status and future trends', *J Solid State Electrochem.*, 2009, **13**, pp. 3–25

[6] Wang L., Kumar R.V.: 'A novel carbon dioxide gas sensor based on solid bielectrolyte', *Sens. Actuators B*, 2003, **88**, pp. 292–299

[7] Nafe H., Aldinger F.: 'CO_2 sensor based on a solid state oxygen concentration cell', *Sens. Actuators B*, 2000, **69**, pp. 46–50

doi: 10.1049/mnl.2016.0240

[8] Sadaoka Y. 'NASICON based CO_2 gas sensor with an auxiliary electrode composed of Li_2CO_3-metal oxide mixtures', *Sens. Actuators B*, 2007, **80**, pp. 234–242
[9] Miura N., Yao S., Sato M., Shimizu Y., Kuwata S., Yamazoe N.: 'Carbon-dioxide sensor using combination of fluoride-ion conductor and metal carbonate', *Chem. Lett.*, 1993, **11**, pp. 1973–1976
[10] Wang H., Ren J., Zhang H., Sun G., Jiang Z.: 'Solid potentiometric CO_2 sensor using Li_3PO_4 film as the electrolyte', *IEEE Sens. J.*, 2012, **12**, pp. 2001–2005
[11] Satyanarayana L., Noh W.S., Kim G.H., Lee W.Y., Park J.S.: 'A low temperature potentiometric CO_2 sensor combined with SiO_2:B_2O_3:Li_2O:Bi_2O_3 composite metal oxide', *IEEE Sens. J.*, 2008, **8**, (9–10), pp. 1565–1570
[12] Satyanarayana L., Choi G.P., Noh W.S., Lee W.Y., Park J.S.: 'Characteristics and performance of binary carbonate auxiliary phase CO_2 sensor based on Li_3PO_4 solid electrolyte', *Solid State Ion*, 2007, **177**, pp. 3485–3490
[13] Lee C., Akbar S.A., Park C.O.: 'Potentiometric CO_2 gas sensor with lithium phosphorous oxynitride electrolyte', *Sens. Actuators B*, 2001, **80**, pp. 234–242
[14] Jeong C., Song H.G., Chang D.R., Kim H.S.: 'Fabrication of the planar-type CO_2 gas sensor using an evaporated Li_3PO_4 film and its sensing characteristics', *Met. Mater. Int.*, 2009, **15**, pp. 101–105
[15] Noh W.S., Satyanarayana L., Park J.S.: 'Potentiometric CO_2 sensor using Li+ ion conducting Li_3PO_4 thin film electrolyte', *Sensors*, 2005, **5**, pp. 465–472
[16] Li P., Sun G., Wang H., Jiang Z.: 'Fabrication of thin film potentiometric CO_2 sensors on differentiate substrate surfaces and their characteristics', *Micro Nano Lett.*, 2013, **8**, pp. 445–449
[17] Lee H.K., Choi N.J., Moon S.E., Yang W.S., Kim J.: 'A solid electrolyte potentiometric CO_2 gas sensor composed of lithium phosphate as both the reference and the solid electrolyte materials', *J.ournal of the Korean Phys. Soc.*, 2012, **61**, pp. 938–941
[18] Choi N.J., Lee H.K., Moon S.E., Yang W.S., Kim J.: 'Stacked-type potentiometric solid-state CO_2 gas sensor', *Sens. Actuators B.*, 2013, **187**, pp. 340–346
[19] Menil F., Daddah B.O., Tardy P., Debeda H., Lucat C.: 'Planar LiSICON-based potentiometric CO_2 sensors: influence of the working and reference electrodes relative size on the sensing properties', *Sens. Actuators B.*, 2005, **107**, pp. 695–707